Journal of Power Sources 183 (2008) 325–329

Contents lists available at ScienceDirect

Journal of Power Sources

journal homepage: www.elsevier.com/locate/jpowsour

Short communication

Electrochemical characteristics of manganese oxide/carbon composite as a cathode material for Li/MnO_2 secondary batteries

Jungbae Lee[a], Jae-Myung Lee[a], Sukeun Yoon[a], Sang-Ok Kim[a], Jung-Soo Sohn[b], Kang-In Rhee[b], Hun-Joon Sohn[a,*]

[a] Department of Materials Science and Engineering, Research Center for Energy Conversion and Storage, Seoul National University, San 56-1 Sillim-Dong, Kwanak-Gu, Seoul 151-742, Republic of Korea
[b] Minerals and Materials Processing Division, Korea Institute of Geoscience & Mineral Resources, Daejeon 305-350, Republic of Korea

ARTICLE INFO

Article history:
Received 22 January 2008
Received in revised form 4 March 2008
Accepted 29 April 2008
Available online 9 May 2008

Keywords:
Lithium-ion batteries
Cathode
Electrolytic manganese dioxide
Carbon composite
Irreversible capacity
Cycleability

ABSTRACT

Electrolytic manganese dioxide (EMD) recovered from a simulated leaching solution of spent alkaline batteries using a modified cyclone cell is tested as a cathode material for Li secondary batteries. An EMD/C(Super P) composite heat-treated at 400 °C after high-energy mechanical milling shows better electrochemical performance than that of pure EMD in terms of cycleability and capacity fading. The electrochemical characteristics of the EMD/C(Super P) composite are investigated by various analytical techniques. The irreversible capacity during the first cycle is mainly due to the formation of a Li_2MnO_3 phase. The carbon composite also retards the dissolution of Mn during cycling.

1. Introduction

The demand for a secondary battery with high-specific energy increases with the advancement of electronic devices. Accordingly, the research and development of secondary lithium batteries has intensified. The lithium-ion battery is relatively safe and has a long cycle-life. At present, $LiCoO_2$ is used as the cathode material in commercial Li-ion batteries. However, it still suffers from some disadvantages such as high cost, toxicity and limited sources of cobalt ore. Among the candidates for the cathode, one of the most attractive materials to replace $LiCoO_2$ is a layered-structured manganese oxide including the spinel type since the cost of manganese oxide is inexpensive, non-toxic, high-voltage material and offers various polymorphic modifications [1–3]. In view of these respects, manganese dioxide-based materials have been studied intensively as alternative cathodes for lithium-ion batteries. Spinel $LiMn_2O_4$ exhibits low capacity and the capacity decreases rather rapidly with cycling, especially when cells are subjected to deep discharge cycles [4]. Various layer compounds have been examined with regard to their electrochemical characteristics, crystal structures, physical properties [5,6]. Also the effect of carbon additives on the extent of solvent oxidation, spinel dissolution and capacity fading have been investigated in a Li/$Li_xMn_2O_4$ cell [7,8]. Lithium–manganese dioxide (Li/MnO_2) batteries have used MnO_2 as a cathode active material, and MnO_2 has already been employed in alkaline manganese batteries [9,10].

Industrially, MnO_2 is obtained by anodic oxidation of manganese sulfate on an inert anodic substrate in hot sulfuric acid [11]. In this work, using electrolytic manganese dioxide (EMD) recovered from a simulated leaching solution of spent alkaline batteries using a modified cyclone cell is investigated as the positive material for a high-voltage, inexpensive lithium secondary battery. In order to improve the cycleability of EMD, an EMD/C(Super P) composite has been formulated and investigated.

2. Experimental

An electrochemical reactor, utilizing the principal features of the well-known hydrocyclone, was employed for the recovery of manganese dioxide from dilute acidic solution. In our previous studies [12,13], Pd and Pt were recovered much more effectively using a modified cyclone reactor compared with the existing facilities, and the cell was described in detail. Reagent grade, manganese sulfate powder ($MnSO_4 \cdot H_2O$, ≥98%, Aldrich) was dissolved in

* Corresponding author. Tel.: +82 2 880 7226; fax: +82 2 885 9671.
E-mail address: hjsohn@snu.ac.kr (H.-J. Sohn).

0378-7753/$ – see front matter © 2008 Elsevier B.V. All rights reserved.
doi:10.1016/j.jpowsour.2008.04.084

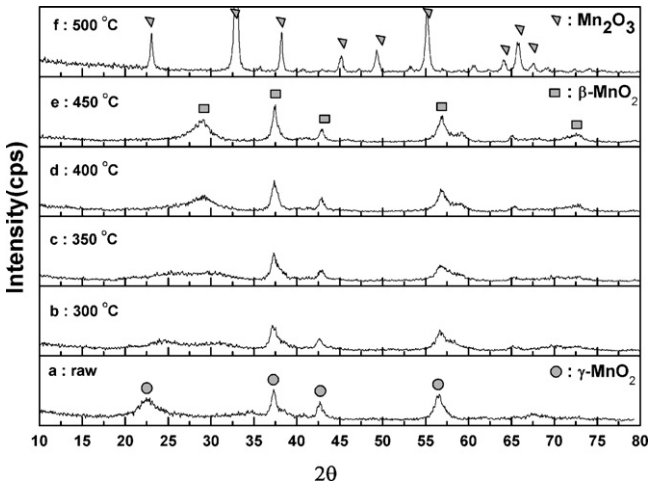

Fig. 1. XRD patterns for EMD heat-treated at various temperatures: (a) raw, (b) 300 °C, (c) 350 °C, (d) 400 °C, (e) 450 °C, and (f) 500 °C.

distilled water and the pH was adjusted with sulfuric acid. All the experiments were performed at 95 °C, $[Mn^{2+}] = 5\,kg\,m^{-3}$, pH 3.5, flow rate = $0.000265\,m^3\,s^{-1}$ and under galvanostatic conditions at an applied current of 1 A.

The manganese dioxide was recovered, washed with distilled water, and then dried under vacuum for 12 h at 120 °C. An EMD/C(Super P) composite with a weight ratio of 95:5 was prepared via the following two steps. For high-energy mechanical milling, a vial was assembled in an argon-filled glove-box and mounted on a SPEX-8000 vibratory mill. The mixture was milled at 500 rpm for 1 h to synthesize nanocomposite particles of carbon dispersed in the MnO_2 matrix followed by heat-treatment in air between 350 and 500 °C. The characteristics of powder samples were identified by X-ray diffraction (XRD; Rigaku, D/MAX 2500/PC series). X-ray photoelectron spectroscopy (XPS; Kratos, Axis) with monochromatic Al Kα (1486.6 eV) radiation was used to analyze the chemical binding energies of the samples. The concentration of metal ions in the electrolyte was quantified in a inductively coupled plasma-emission spectrometer (Shimadzu, JP/ICPS-7500). A high-resolution transmission electron microscope (HR-TEM; JEOL, JEM-3010) was employed to identify the phases formed during cycling.

The electrodes were prepared by coating slurries of active material powders (80 wt%), Super P (10 wt%) and polyvinylidine fluoride (PVDF, 10 wt%) dissolved in *N*-methyl pyrrolidinone (NMP) on aluminum foil substrates. After coating, the electrodes were pressed and dried for 4 h at 120 °C. The electrodes were cut into discs (10 mm in diameter and about 200 μm in thickness). Coin-type test cells were assembled in an argon-filled glove-box and used Celgard 2400

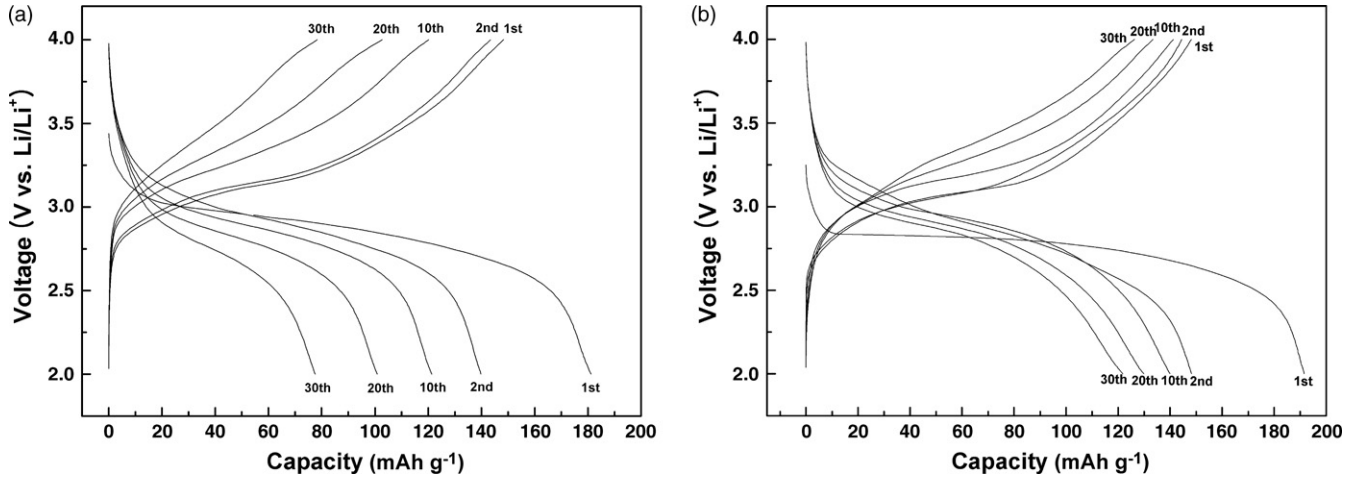

Fig. 2. Voltage profile of (a) γ-MnO_2 and (b) β-MnO_2/C composite at a constant current rate of 20 mA g^{-1}.

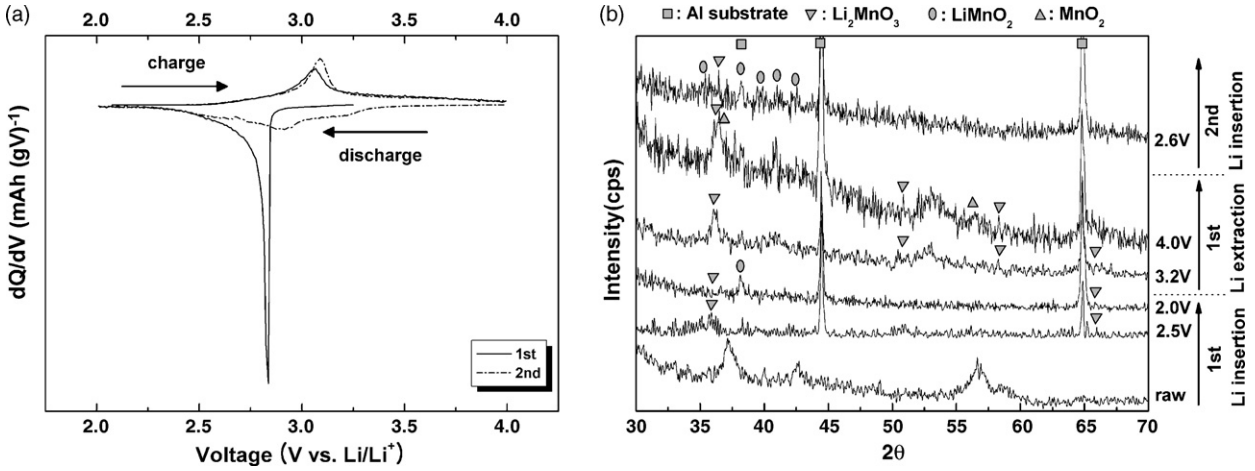

Fig. 3. (a) DCP of β-MnO_2/C composite; (b) ex situ XRD patterns of β-MnO_2/C composite electrode.

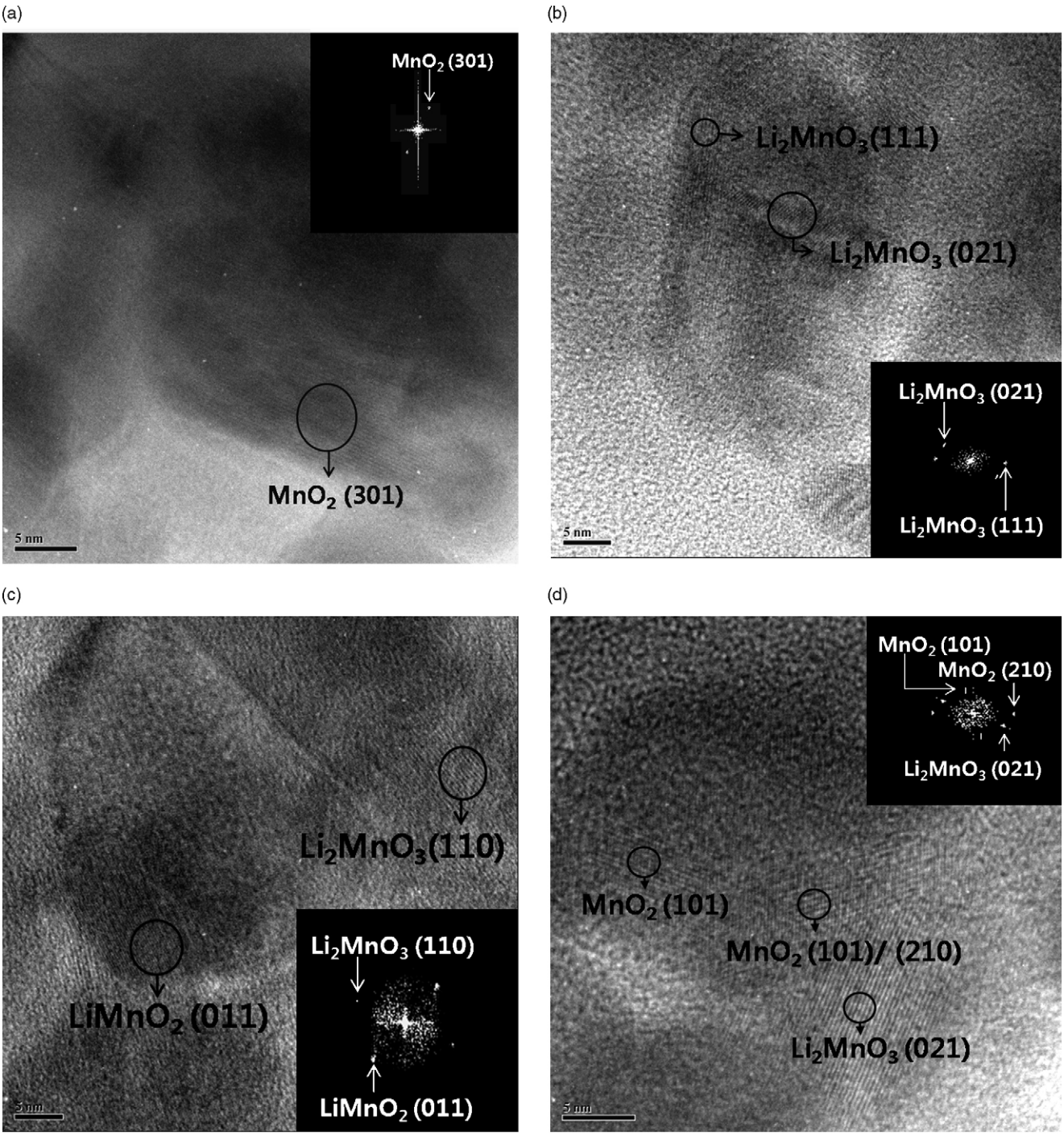

Fig. 4. HR-TEM images of (a) raw β-MnO_2/C, (b) at 2.5 V during first discharge, (c) at 2.0 V during first discharge, and (d) at 4.0 V during first charge.

as a separator, 1 M $LiPF_6$ in ethylene carbonate (EC)/diethyl carbonate (DEC) (1:1 volume ratio, Cheil Industries) as an electrolyte, and Li foil as a counter electrode. Discharge (Li insertion)/charge (Li extraction) experiments were performed galvanostatistically within a voltage window of 2.0–4.0 V (vs. Li/Li^+) and at a current density of 20 mA g^{-1}.

3. Results and discussion

The XRD patterns of EMD powder samples recovered from the modified cyclone cell and from samples heat-treated at various temperatures are shown in Fig. 1. The as-recovered samples show the typical characteristics of EMD (Fig. 1a) which is γ-MnO_2. A phase change from γ-MnO_2 to β-MnO_2 ($P4_2/mnm$) is observed, as expected, when the samples are heat-treated above 300 °C [14]. The diffraction peaks become sharp with temperature up to 450 °C (Fig. 1b–e). Finally, the sample heat-treated at 500 °C (Fig. 1f) corresponds to the Mn_2O_3 phase, into which Li cannot be inserted.

Preliminary tests were performed and the β-MnO_2/C composite heat-treated at 400 °C shows the best electrochemical performance compared with composites heat-treated between 300 and 450 °C

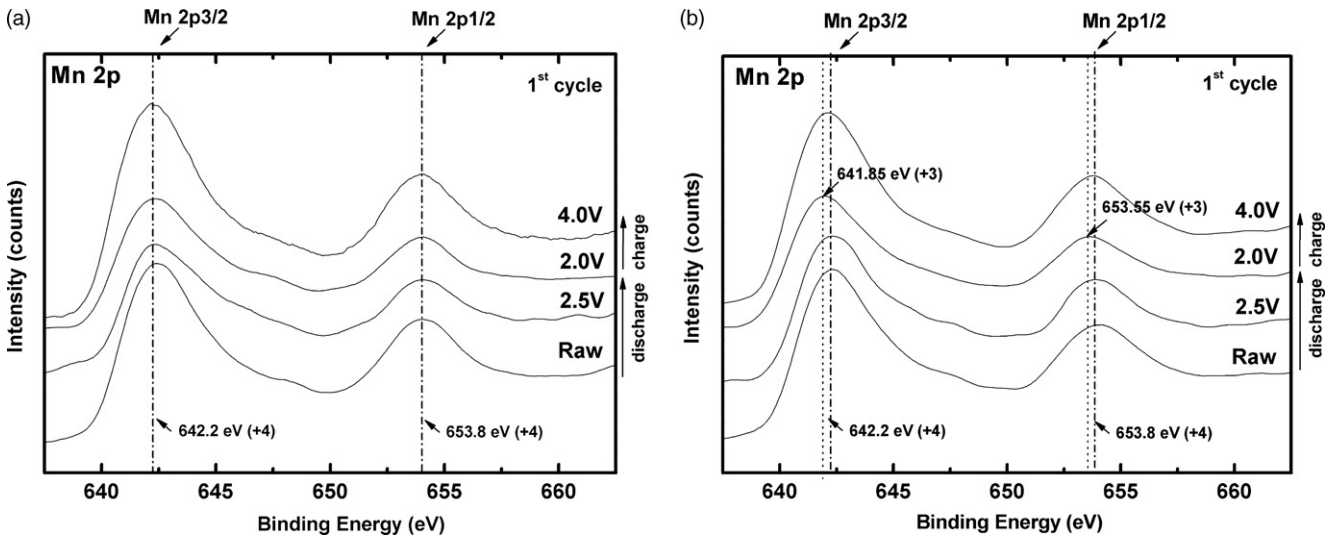

Fig. 5. XPS spectra of Mn 2p for β-MnO_2/C electrode during first cycle. (a) and (b) indicate different locations.

in terms of capacity and cycleability. The voltage profiles and the specific discharge and charge capacities of pure γ-MnO_2 and the β-MnO_2/C composite heat-treated at 400 °C at various stages of cycling are shown in Fig. 2. During the discharge reaction, Li ions are inserted into γ-MnO_2 which has a tunnel structure. The hexagonally close-packed arrangement is distorted during lithium insertion, and capacity fades rapidly upon cycling, as evidenced in Fig. 2(a) [15]. For β-MnO_2/C composite heat-treated at 400 °C, a long plateau at 2.83 V (vs. Li/Li^+) is observed and indicates a phase change during the first discharge reaction. Although the first discharge capacity is almost the same as that of γ-MnO_2, capacity retention is better. The β-MnO_2 active material tested here can be considered to have a low crystallinity since it shows rather broad X-ray diffraction patterns, as can be seen in Fig. 1e. It has been reported [16] that β-MnO_2 active material with a low crystallinity yields more discharge capacity than that with a well-developed crystalline structure.

A differential capacity plot (DCP) of the β-MnO_2/C composite heat-treated at 400 °C is presented in Fig. 3(a). In addition, ex situ X-ray diffraction patterns at various potentials during the first cycle are given in Fig. 3(b). The plateau shown in Fig. 2(b) corresponds to a sharp peak at 2.83 V in the DCP. When the potential is lowered to 2.5 V, β-MnO_2 disappears and Li_2MnO_3 appears, followed by the formation of $LiMnO_2$ at 2.0 V as shown in Fig. 4(b).

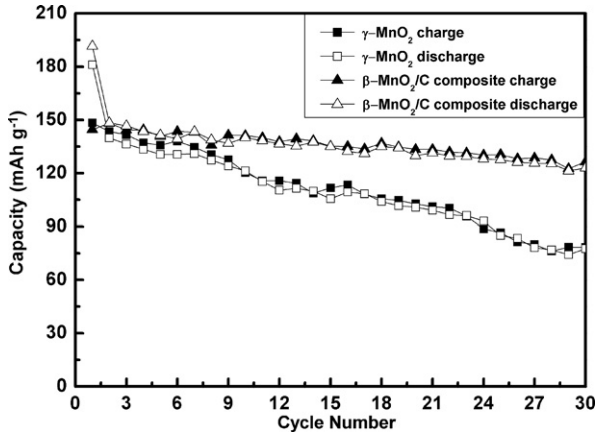

Fig. 6. Comparison of cycle performances of γ-MnO_2 and β-MnO_2/C composite.

During the first charge, Li is extracted and the β-MnO_2 phase appears again with the remaining Li_2MnO_3 phase, which is considered to be inactive [17,18]. After the second discharge, $LiMnO_2$ is the dominant phase and co-exists with the Li_2MnO_3 phase formed previously.

HR-TEM analyses (Fig. 4) support the above results. The results for the β-MnO_2/C composite before Li insertion are given in Fig. 4(a), whereas Fig. 4(b) shows that the Li_2MnO_3 phase is formed when lithium is inserted at 2.5 V during the first discharge reaction. At 2.0 V, the $LiMnO_2$ phase appears and co-exists with Li_2MnO_3 phase, as shown in Fig. 4(c). When Li is extracted at 4.0 V, $LiMnO_2$ returns to β-MnO_2 and the Li_2MnO_3 formed during the first discharge remains (Fig. 4(d)).

XPS spectra recorded at two different locations on the electrode (Fig. 5) shows that two oxidation states of Mn, i.e., Mn^{4+}/Mn^{3+}, exist at 2.0 V during the first discharge, from which both Li_2MnO_3 (Mn^{4+}) and $LiMnO_2$ (Mn^{3+}) phases co-exist as the final products. When Li is extracted (4.0 V) during the first charge, the spectra show that only the Mn^{4+} state is present since the valence of Mn is tetravalent for both remaining Li_2MnO_3 and MnO_2 phases. Based on the above analyses, the irreversible capacity is mainly due to the formation of the Li_2MnO_3 phase during the first cycle.

The cycleability of γ-MnO_2 and the β-MnO_2/C composite between 2.0 and 4.0 V is presented in Fig. 6. The discharge capacity of γ-MnO_2 falls from an initial 181 to 140 mAh g^{-1} with a Coulombic efficiency of 78% for the first cycle and then declines to 77 mAh g^{-1} after 30 cycles. The γ-MnO_2/C composite with a discharge capacity of 190 mAh g^{-1} initially and 121 mAh g^{-1} after 30 cycles shows better capacity retention. One mechanism of capacity fading is the dissolution of Mn in the electrolyte during cycling [5,19]. The dissolution of Mn is generally attributed to the existence of HF, which is easily formed when using $LiPF_6$ as the electrolyte salt. The correlation between HF formation and dissolution of Mn has been

Table 1
ICP analyses of Mn in electrolyte[a] after 30 cycles

Test sample	Mn concentration (ppm)
EMD (raw)	1.6016
EMD/C composite[b]	0.4199

[a] EC:DEC (1:1, vol.) with 1 M $LiPF_6$.
[b] HTT at 400 °C after mechanical alloying.

reported [20], and $LiPF_6$ itself contains a small amount of HF during the manufacturing process [21]. The amounts of Mn dissolved in the electrolyte after 30 cycles were measured and are summarized in Table 1. It shows that the carbon composite effectively retards the dissolution of Mn from the electrode during cycling to give improved capacity retention.

4. Conclusions

In this study, β-MnO_2/C composites are prepared by mechanical milling followed by heat-treatment, and then tested as cathodes for Li secondary batteries. Through ex situ XRD, XPS and HR-TEM analyses, it is found that the irreversibility after the first discharge reaction is mainly due to the formation of an inactive Li_2MnO_3 phase. The composite displays better electrochemical performance compared with that of pure γ-MnO_2 recovered from a simulated leaching solution. This behaviour is due to the composite effectively retarding the dissolution of Mn into the electrolyte.

Acknowledgements

The work was supported by the Resource Recycling R&D Centre in Korea and the Korea Science and Engineering Foundation (KOSEF) through the Research Center for Energy Conversion and Storage at Seoul National University (Grant no. R11-2002-102-02001-0).

References

[1] C.S. Johnson, J. Power Sources 165 (2007) 559.
[2] C.S. Johnson, M.F. Mansuetto, M.M. Thackeray, Y. Shao-Horn, S.A. Hackney, J. Electrochem. Soc. 144 (1997) 2279.
[3] W. Wang, M. Wu, X. Liu, J. Solid State Chem. 164 (2002) 5.
[4] S. Yamada, T. Ohski, K. Inada, N. Chiba, H. Nose, T. Uchida, Proc. Rechargeable Lithium Batteries, PV 90-5, The Electrochemical Society, Pennington, NJ, 1990, p. 21.
[5] M.S. Whittingham, J. Electrochem. Soc. 123 (1976) 315.
[6] D.W. Murphy, F.A. Trumhore, J.N. Carides, J. Electrochem. Soc. 124 (1977) 325.
[7] D.H. Jang, S.M. Oh, Electrochim. Acta 43 (1998) 1023.
[8] J. Kim, B. Kim, J.-G. Lee, J. Cho, B. Park, J. Power Sources 139 (2005) 289.
[9] H. Ikeda, T. Saito, H. Tamura, in: Manganese Dioxide Symposium, vol. 1, Cleveland Section of the Electrochemical Society Inc., 1977.
[10] H. Ikeda, T. Saito, H. Tamura, Denki Kagaku 45 (1977) 314.
[11] R.P. Williams, PhD Thesis, University of New Castle, 1996.
[12] S.-K. Kim, C.K. Lee, J.-C. Lee, K.-I. Rhee, H.-J. Sohn, T. Kang, Resources Process, 51 (2004-spring) 1.
[13] Y.-U. Kim, H.-W. Cho, H.-S. Lee, C.-K. Lee, J.-C. Lee, K.-I. Rhee, H.-J. Sohn, T. Kang, J. Appl. Electrochem. 32 (2002) 1235.
[14] Y. Chabre, J. Pannetier, Prog. Solid State Chem. 23 (1995) 1.
[15] M.M. Thackeray, Prog. Solid State Chem. 25 (1997) 1.
[16] M.M. Thackeray, Prog. Batt. Batt. Mater. 14 (1995) 1.
[17] T. Nohma, T. Saito, N. Furukawa, H. Ikeda, J. Power Sources 26 (1989) 389.
[18] M.M. Thackeray, C.S. Johnson, J.T. Vaughey, N. Li, S.A. Hackney, J. Mater. Chem. 15 (2005) 2257.
[19] J.H. Lee, J.K. Hong, D.H. Jang, Y.-K. Sun, S.M. Oh, J. Power Sources 46 (2000) 541.
[20] A.D. Pasquier, A. Blyr, P. Courjal, D. Larcher, G. Amatucci, B. Gerand, J.M. Tarascon, J. Electrochem. Soc. 146 (1999) 428.
[21] G.G. Amatucci, A. Blyr, C. Sigala, P. Alfonse, J.M. Tarascon, Solid State Ionics 104 (1997) 13.